

# Perturbation Analysis of Variable Density Flow in Porous Media

By M. DENTZ<sup>1</sup>, D.M. TARTAKOVSKY<sup>2</sup>, E. ABARCA<sup>1</sup>,  
A. GUADAGNINI<sup>3</sup>, X. SANCHEZ-VILA<sup>1</sup>  
AND J. CARRERA<sup>1</sup>

<sup>1</sup>Department of Geotechnical Engineering and Geosciences, Technical University of Catalonia (UPC), Barcelona, Spain

<sup>2</sup>Theoretical Division, Los Alamos National Laboratory, Los Alamos, New Mexico 87545, USA

<sup>3</sup>DIAR, Politecnico di Milano, Piazza L. da Vinci, 32, 20133, Milano, Italy

(Received 22 February 2005 and in revised form ??)

Steady-state distributions of water potential and salt concentration in coastal aquifers are typically illustrated by the Henry problem, which consists of a fully coupled system of flow and transport equations. Coupling is caused by the dependence of water density on salt concentration. While the Henry problem often serves as a benchmark for numerical codes, the accuracy of the existing numerical and approximate analytical solutions is hard to gauge. We provide a closed form formulation of the flow problem in terms of salt concentration and use a perturbation expansion in the coupling parameter to solve it analytically. The perturbation procedure results in a recursive set of flow and transport equations and their solutions that effectively decouples the two processes. This decoupling approach can be applied to a range of problems involving variable density fluids and sheds new light on coupled flow and transport mechanisms.

---

## 1. Introduction

Variable density flow and transport in porous media have received increasing attention in the literature. A reason for such interest is that fluid density variations appear in many relevant environmental problems. One of the most significant environmental problems is that of pollution of freshwater bodies by water with high concentrations of salts in dissolution. Salty water can come either from the sea (e.g., Custodio *et al.* 1987) or from natural occurring brines (e.g., Schelkes *et al.* 2001; Herbert *et al.* 1988). High density water can also result from landfill leachate and irrigation practices (e.g., Simmons *et al.* 2002). Another area of interest falling under the purview of variable density flows is the problem of pollution by non-aqueous phase liquids (e.g., Taylor *et al.* 2001). In all these problems one is concerned with flow in the shallow subsurface. Other studies deal with density-driven flow in the deep subsurface, where density differences are caused mainly by temperature or pressure. These variations can be both natural and anthropogenic. One example of the latter arises from nuclear fuel waste heat generation, which renders the study of variable-density flow relevant to performance assessment analyses (e.g., Ophori 2004; Yang & Edwards 2000).

It is well known that variable-density flows in porous media can become unstable. Instabilities and fingering develop when a denser fluid lies above a lighter fluid (e.g., Manickam & Homsy 1995; Wooding *et al.* 1997). When lighter water is on top, flow is

stable and mixing is caused by diffusive and/or dispersive mechanisms (e.g., Huppert & Woods 1995). This is the flow scenario that usually occurs during seawater intrusion into coastal aquifers (e.g., Alkalali & Rostron 2003) and is the subject of this study. This problem poses significant environmental and economical challenges around the world (Panday *et al.* 1993; Smith & Turner 2001; Aliewi *et al.* 2001; Paniconi *et al.* 2001) and has important water resources management implications.

Seawater intrusion has been traditionally described by two alternative mathematical models. The first approach assumes that a sharp interface separates the body of fresh water from the intruding saltwater. By ignoring the existence of a transition zone, this approach recasts the problem in terms of potential theory for interface propagation. The use of its tools, such as conformal mapping, has led to a number of analytical solutions (e.g., Bear & Dagan 1964; Huppert & Woods 1995; Naji *et al.* 1998; Kacimov & Obnosov 2001), which provide invaluable insights into the phenomenon. There exist, however, a plethora of physical conditions for which the width of the transitional zone cannot be neglected. This is especially so since even minute concentration of salt can make fresh water undrinkable.

The second approach, which we adopt here, accounts for the presence of the transition zone resulting from the dynamic equilibrium of moving fresh- and saltwater. The corresponding mathematical model consists of a system of the variable-density (Darcy) flow equation and the advection-dispersion/diffusion equation. The two governing equations are fully coupled through the dependence of water density on salt concentration.

The intrinsic complexity of the coupled governing equations precludes the development of closed form analytical solutions even for simple geometries and simple boundary conditions. This, in turn, has led to the proliferation of numerous numerical codes, many of which are reviewed in Bear *et al.* (1999). The absence of analytical solutions and the relative scarcity of experimental data (Schincariol & Schwartz 1990; Oltean *et al.* 2004) complicates the establishment of benchmark problems for testing the accuracy and robustness of these numerical codes. Instead, numerical solutions are compared with each other, and the differences between them can be quite significant (Croucher & O’Sullivan 1995). Therefore, there is a need to provide analytical solutions for specific problems that can be used for benchmarking (Weatherill *et al.* 2004).

This study is devoted to the analysis of the Henry problem (Henry 1964), which, despite some reservations (Simpson & Clement 2003), remains one of the most widely used benchmark problems. The importance of the Henry problem goes beyond benchmarking, since it provides physical insight into transport processes associated with seawater intrusion (Abarca *et al.* 2004). Available quasi-analytical solutions of the Henry problem (Henry 1964; Segol 1994) are based on a Galerkin method and are rendered impractical by their slow rates of convergence. Typically, the Henry problem is solved numerically (Pinder & Cooper 1970; Segol *et al.* 1975; Galeati *et al.* 1992; Segol 1994), leading to quantitatively different solutions (Croucher & O’Sullivan 1995).

In the present study we present a new methodology for the analytical solution the Henry problem and other similar problems describing variable-density flows in porous media. Section 2 contains a mathematical formulation of the Henry problem and introduces relevant dimensionless parameters. In Section 3, we provide an exact solution for the flow problem as a functional of the salt concentration and derive an integral equation for the salt concentration. These serve as a basis for a perturbation solution of the fully coupled system of variable-density flow equations, which we derive in Section 4. The accuracy and convergence rate of this perturbation expansion are examined in Section 5, which also contains a discussion on the importance of coupling.

## 2. Henry Problem: Steady-State Flow and Transport

### 2.1. Problem Formulation

The Henry formulation of seawater intrusion describes the steady-state position of a diffused salt-water wedge within a confined aquifer balanced against a flowing fresh-water field. Within this framework, fluid flow in porous media is governed by the modified Darcy law (e.g., Bear 1972),

$$\mathbf{u} = -\frac{k}{\mu} \{\nabla p + \rho g \mathbf{e}_3\}, \quad (2.1)$$

where  $\mathbf{u}$  is the fluid flux,  $k$  is the intrinsic permeability of the porous medium,  $\mu$  is the viscosity of the fluid,  $p$  is pressure,  $g$  is gravitational acceleration,  $\rho$  is the concentration-dependent density of the fluid, and  $\mathbf{e}_3$  denotes the unit vector in the vertical direction. In the absence of sources and sinks, fluid continuity in steady state is expressed by

$$\nabla \cdot \{\rho \mathbf{u}\} = 0. \quad (2.2)$$

The fluid density  $\rho$  varies with the salt concentration  $C$ , with the latter satisfying the steady-state advection-diffusion equation, which Henry (1964) wrote as,

$$\nabla \cdot \{\mathbf{u} C - \theta D \nabla C\} = 0, \quad (2.3)$$

where  $D$  is the constant diffusion coefficient. Both permeability  $k$  and porosity  $\theta$  are constant for homogeneous porous media.

Equations (2.1) – (2.3) are closed by specifying a constitutive relationship  $\rho = \rho(C)$  between fluid density  $\rho$  and salt concentration  $C$ . While a number of such relationships exist (e.g., Holzbecher 1998; Diersch *et al.* 2002), the linear relationship

$$\rho = \rho_f \left(1 + \epsilon \frac{C}{C_s}\right) \quad (2.4)$$

originally used by Henry (Henry 1964) remains the most popular. Here  $C_s$  is the concentration of salt in seawater and  $\epsilon$  denotes the relative density contrast between the densities  $\rho_f$  of freshwater and  $\rho_s$  of saltwater,

$$\epsilon \equiv \frac{\rho_s - \rho_f}{\rho_f}. \quad (2.5)$$

Note that  $C \leq C_s$  and, hence,  $\rho_f \leq \rho \leq \rho_s$ .

The density of freshwater for the usual range of temperatures in aquifers is  $\rho_f = 10^3 \text{ kg/m}^3$ . The density of seawater generally increases with decreasing temperature, increasing salinity, and increasing depth in the ocean. The density of seawater at the surface of the sea/ocean varies (with a few exceptions) between  $1.020$  and  $1.029 \text{ kg/m}^3$ , with a worldwide average value of  $1.025 \text{ kg/m}^3$ . Thus, under typical ocean conditions  $\epsilon = 1/40$ , and the Oberbeck-Boussinesq approximation (e.g., Diersch *et al.* 2002) is usually invoked to replace (2.2) with

$$\nabla \cdot \mathbf{u} = 0. \quad (2.6)$$

A usual justification for this approximation is that in coastal aquifers density gradients are of subleading order and can be neglected. Another, and possibly stronger, justification is that the average direction of flow in shallow coastal aquifers is nearly orthogonal to that of the density gradient, i.e.,  $\mathbf{u} \cdot \nabla \rho \approx 0$ .

The Henry problem (Henry 1964) and its subsequent modifications (Segol 1994; Croucher & O'Sullivan 1995) consider the two-dimensional versions of equations (2.1), (2.3), (2.4), and (2.6), which are defined on the vertical cross-section  $\mathbf{x} \equiv (x_1, x_3)^T \in \Omega$ , where

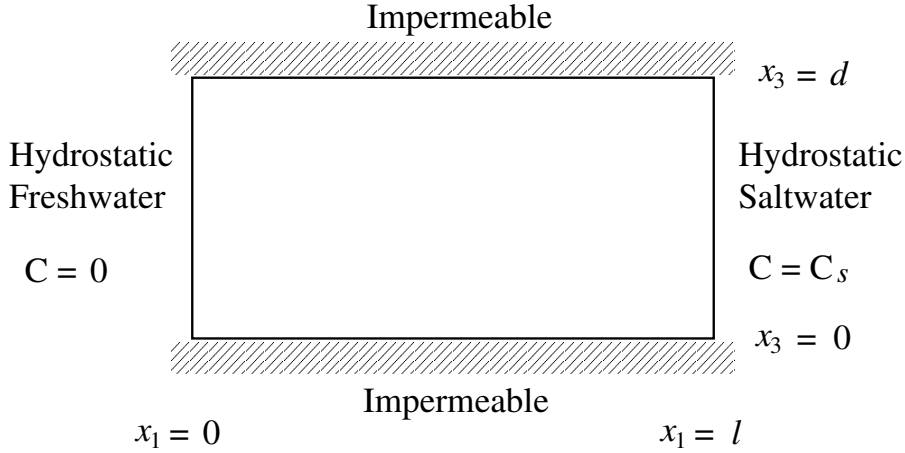


FIGURE 1. Illustration of the flow and transport scenario (after Croucher & O’Sullivan (1995)). Pressure is hydrostatic at the inland ( $x_1 = 0$ ) and sea ( $x_1 = L$ ) boundaries. The salt concentration is zero at the freshwater boundary, and equal to the (constant) concentration  $C_s$  of salt in seawater at the sea boundary. The top and bottom of the domain are impermeable.

$\Omega = [0, L] \times [0, d]$  is a rectangle shown in Figure 1. In this formulation, freshwater enters the confined aquifer  $\Omega$  through an inland boundary  $x_1 = 0$  and discharges into a coastal boundary  $x_1 = L$ . Saltwater from the coastal boundary  $x_1 = L$  advances and mixes with the discharging freshwater, so that a transitional zone from purely fresh- to seawater is formed. At the coastal boundary  $x_1 = L$  a discharge of both freshwater and mixed water takes place. The horizontal boundaries  $x_3 = 0$  and  $x_3 = d$  are assumed to be impermeable to both flow and transport.

The corresponding boundary conditions for flow equations (2.1) and (2.6) are as follows. Fluid pressure  $p(\mathbf{x})$  is prescribed at the freshwater and saltwater boundaries, where it is given by the pressure of hydrostatic saltwater. This yields

$$p(x_1 = 0, x_3) = p_0 - \rho_f g x_3 \quad \text{and} \quad p(x_1 = L, x_3) = \rho_s g (d - x_3), \quad (2.7a)$$

where  $p_0$  is a reference pressure. At the impermeable top and bottom, the vertical component of the Darcian velocity  $\mathbf{u} = (u_1, u_3)^T$  is zero:

$$u_3(x_1, x_3 = 0) = 0 \quad u_3(x_1, x_3 = d) = 0. \quad (2.7b)$$

The boundary conditions for transport equation (2.3) are as follows. At the freshwater and sea boundaries the salt concentration

$$C(x_1 = 0, x_3) = 0, \quad C(x_1 = L, x_3) = C_s, \quad (2.8a)$$

respectively. At the impermeable boundaries at the top and the bottom of the transport domain, mass flux is zero:

$$\frac{\partial C(x_1, x_3 = 0)}{\partial x_3} = 0 \quad \frac{\partial C(x_1, x_3 = d)}{\partial x_3} = 0. \quad (2.8b)$$

Note that the existence of a steady-state regime described by the Henry model requires that the freshwater-saltwater interface be in dynamical equilibrium with average global sea levels, and that the variations in the total flowing freshwater be negligible.

Henry (1964) originally formulated his problem in terms of streamfunctions. He implicitly forced the inland boundary to represent hydrostatic pressure by forcing the gradient

of the streamfunction to be parallel to the boundary, but he did not specify the reference pressure. Instead, he specified the total flow rate across the freshwater boundary. Obviously there is a bijective monotonic relationship between  $p_0$  and the total flow rate. Therefore our formulation is equivalent to Henry's. Specifically, neither of them implies a uniform freshwater flux across the boundary as used by many numerical solutions. In fact, one should expect the freshwater flux to be slightly larger at the top than at the bottom of the boundary. While this difference should be small for most problems, it must be kept in mind when doing detailed comparisons.

### 2.2. Freshwater Head Formulation

We start our analysis by reformulating the generalized Darcy law (2.1) in terms of the equivalent freshwater hydraulic head

$$h = \frac{p}{\rho_f g} + x_3. \quad (2.9)$$

Substituting (2.4) and (2.9) into (2.1) gives

$$\mathbf{u} = -K \left( \nabla h + \mathbf{e}_3 \epsilon \frac{C}{C_s} \right), \quad K \equiv \frac{k \rho_f g}{\mu}, \quad (2.10)$$

where  $K$  is the hydraulic conductivity of a porous medium. Combining (2.6) and (2.10) yields the flow equation written in terms of the freshwater head  $h$ ,

$$\nabla^2 h = -\frac{\epsilon}{C_s} \frac{\partial C}{\partial x_3}. \quad (2.11)$$

In terms of hydraulic head (2.9), boundary conditions (2.7a) and (2.7b) are recast as

$$h(x_1 = 0, x_3) = \frac{p_0}{\rho_f g} \equiv h_0, \quad h(x_1 = L, x_3) = d + \epsilon(d - x_3), \quad (2.12a)$$

and

$$\frac{\partial h(x_1, x_3 = 0)}{\partial x_3} = -\epsilon \frac{C(x_1, x_3 = 0)}{C_s}, \quad \frac{\partial h(x_1, x_3 = d)}{\partial x_3} = -\epsilon \frac{C(x_1, x_3 = d)}{C_s}, \quad (2.12b)$$

respectively.

Substituting (2.6) and (2.10) into (2.3) leads to the steady-state transport equation expressed in terms of the freshwater head  $h$ ,

$$K \nabla h \cdot \nabla C + K \frac{C}{C_s} \frac{\partial C}{\partial x_3} + \theta D \nabla^2 C = 0. \quad (2.13)$$

Equation (2.13) is subject to the boundary conditions (2.8).

### 2.3. Dimensionless Form of the Governing Equations

Next, we recast the governing equations (2.11) and (2.13) in a dimensionless form. Let  $\boldsymbol{\xi} = (\xi_1, \xi_3)^T$  denote a rescaled (dimensionless) spatial position vector and  $\zeta$  an aperture,

$$\xi_1 = \frac{x_1}{L}, \quad \xi_3 = \frac{x_3}{L}, \quad \zeta = \frac{d}{L}, \quad (2.14)$$

respectively. This transformation maps the flow domain  $\Omega = [0, L] \times [0, d]$  onto  $\Omega_d = [0, 1] \times [0, \zeta]$ . From now on,  $\nabla$  is understood to operate with respect to the non-dimensional coordinates  $\boldsymbol{\xi}$ . Dimensionless freshwater hydraulic head  $H$  and salt concentration  $c$  are defined by,

$$H(\boldsymbol{\xi}) = \frac{h(L\boldsymbol{\xi}) - d}{\Delta h_0} \quad \text{and} \quad c(\boldsymbol{\xi}) = \frac{C(L\boldsymbol{\xi})}{C_s}, \quad (2.15)$$

where

$$\Delta h_0 = h_0 - d \quad (2.16)$$

is the global head difference imposed by the inland and sea boundaries in the absence of density effects. Finally, we introduce the dimensionless parameters,

$$\alpha = \frac{\epsilon L}{\Delta h_0}, \quad \beta = \frac{\theta D}{K \Delta h_0}. \quad (2.17)$$

Then the flow problem (2.11) and (2.12) becomes

$$\nabla^2 H(\boldsymbol{\xi}) = -\alpha \frac{\partial c(\boldsymbol{\xi})}{\partial \xi_3} \quad (2.18)$$

subject to boundary conditions

$$H(0, \xi_3) = 1, \quad H(1, \xi_3) = \alpha (\zeta - \xi_3), \quad (2.19a)$$

$$\frac{\partial H(\xi_1, \xi_3 = 0)}{\partial \xi_3} = -\alpha c(\xi_1, 0), \quad \frac{\partial H(\xi_1, \zeta)}{\partial \xi_3} = -\alpha c(\xi_1, \zeta), \quad (2.19b)$$

and the transport problem (2.13) and (2.8) becomes

$$\nabla H(\boldsymbol{\xi}) \cdot \nabla c(\boldsymbol{\xi}) + \alpha c(\boldsymbol{\xi}) \frac{\partial c(\boldsymbol{\xi})}{\partial \xi_3} + \beta \nabla^2 c(\boldsymbol{\xi}) = 0 \quad (2.20)$$

subject to the boundary conditions

$$c(0, x_3) = 0, \quad c(1, x_3) = 1, \quad (2.21a)$$

$$\frac{\partial c(\xi_1, \xi_3 = 0)}{\partial \xi_3} = 0, \quad \frac{\partial c(\xi_1, \xi_3 = \zeta)}{\partial \xi_3} = 0. \quad (2.21b)$$

It now becomes apparent that the Henry problem for seawater intrusion in coastal aquifers (2.18) – (2.21) is completely characterized by the dimensionless parameters  $\alpha$  and  $\beta$  in (2.17). The coupling parameter  $\alpha$  is the ratio of the characteristic velocity induced by density effects,  $K \epsilon$ , to the flow velocity in the absence of density effects,  $K \Delta h_0 / L$ . The strength of coupling between the flow and salt transport processes increases with  $\alpha$ . The Peclet number  $\beta$  compares the strength of diffusion,  $D$ , to a typical total flux per unit length in the absence of density effects,  $K \Delta h_0 L / \theta$ .

### 3. Green Function Solutions

In the following, we derive an exact solution for the flow problem (2.18) – (2.19) as a functional of the salt concentration  $c(\boldsymbol{\xi})$ , and an integral equation for the salt concentration, which serve as a basis for a perturbation solution for the fully coupled system of flow and transport equations.

#### 3.1. Solution of the Flow Problem

Let  $G(\boldsymbol{\xi}, \boldsymbol{\xi}')$  be the Green's function for the flow problem (2.18) – (2.19) defined as the solution of the Poisson equation

$$\nabla^2 G(\boldsymbol{\xi}, \boldsymbol{\xi}') = -\delta(\boldsymbol{\xi} - \boldsymbol{\xi}'), \quad (3.1a)$$

where  $\delta(\boldsymbol{\xi})$  is the Dirac delta function, subject to the homogeneous boundary conditions

$$G|_{\xi_1=0} = G|_{\xi_1=1} = 0, \quad \frac{\partial G}{\partial \xi_3}|_{\xi_3=0} = \frac{\partial G}{\partial \xi_3}|_{\xi_3=\zeta} = 0. \quad (3.1b)$$

Then a formal solution of (2.18) – (2.19) can be written as

$$H(\boldsymbol{\xi}) = \alpha \int_{\Omega_d} G \frac{\partial c}{\partial \xi'_3} d\boldsymbol{\xi}' + \int_{\partial\Omega_d} \left[ \mathbf{e}_3 G \frac{\partial H}{\partial \xi'_3} - \mathbf{e}_1 H \frac{\partial G}{\partial \xi'_1} \right] \cdot d\mathbf{n}, \quad (3.2)$$

where  $\mathbf{n}$  is the unit normal vector for the domain boundary  $\partial\Omega_d$ .

We derive in Appendix A.1 two alternative representations for the Green's function  $G(\boldsymbol{\xi}, \boldsymbol{\xi}')$ . The first representation is given by

$$G(\boldsymbol{\xi}, \boldsymbol{\xi}') = \frac{2}{\pi} \sum_{m=1}^{\infty} \sin(m\pi \xi_1) \sin(m\pi \xi'_1) \cosh(m\pi \xi'_3) \frac{\cosh[m\pi(\zeta - \xi_3)]}{m \sinh(m\pi \zeta)}. \quad (3.3)$$

for  $\xi'_3 < \xi_3$ . For  $\xi'_3 > \xi_3$  the arguments  $\xi_3$  and  $\xi'_3$  are switched in (3.3). The second representation for  $G(\boldsymbol{\xi}, \boldsymbol{\xi}')$  is

$$G(\boldsymbol{\xi}, \boldsymbol{\xi}') = \frac{\xi'_1}{\zeta} (1 - \xi_1) + \frac{2}{\pi} \sum_{n=1}^{\infty} \cos\left(n\pi \frac{\xi_3}{\zeta}\right) \cos\left(n\pi \frac{\xi'_3}{\zeta}\right) \times \\ \sinh\left(\frac{n\pi \xi'_1}{\zeta}\right) \frac{\sinh\left[\frac{n\pi}{\zeta}(1 - \xi_1)\right]}{n \sinh\left(\frac{n\pi}{\zeta}\right)} \quad (3.4)$$

for  $\xi'_1 < \xi_1$ . For  $\xi'_1 > \xi_1$  the arguments  $\xi_1$  and  $\xi'_1$  are switched in (3.4).

We use representation (3.3) to evaluate the first boundary integral on the right side of (3.2) and representation (3.4) to evaluate the second boundary integral. Thus, (3.2) gives a solution for the non-dimensional freshwater head,

$$H(\boldsymbol{\xi}) = (1 - \xi_1) + \alpha \eta_B(\boldsymbol{\xi}) + \alpha \eta_C[\boldsymbol{\xi}, c(\boldsymbol{\xi})], \quad (3.5)$$

where

$$\eta_B = \frac{\xi_1 \zeta}{2} + \sum_{l=1}^{\infty} a_l \cos\left(\frac{l\pi \xi_3}{\zeta}\right) \frac{\sinh\left(\frac{l\pi \xi_1}{\zeta}\right)}{\sinh\left(\frac{l\pi}{\zeta}\right)}, \quad a_l = \frac{2\zeta(1 - (-1)^l)}{l^2 \pi^2} \quad (3.6)$$

is a contribution to  $H$  stemming from the boundary conditions at the saltwater boundary, and

$$\eta_C = \int_{\Omega_d} G \frac{\partial c}{\partial \xi'_3} d\boldsymbol{\xi}' + \sum_{l=1}^{\infty} \frac{1}{l\pi} \frac{\sin(l\pi \xi_1)}{\sinh(l\pi \zeta)} \left\{ b_l^{(1)} \cosh[l\pi(\xi_3 - \zeta)] - b_l^{(2)} \cosh(l\pi \xi_3) \right\}, \quad (3.7a)$$

$$b_l^{(1)} = 2 \int_0^1 c(\xi_1, 0) \sin(l\pi \xi_1) d\xi_1, \quad b_l^{(2)} = 2 \int_0^1 c(\xi_1, \zeta) \sin(l\pi \xi_1) d\xi_1 \quad (3.7b)$$

is a contribution to  $H$  resulting entirely from the coupling of flow and salt transport.

Note that  $\eta_C[\boldsymbol{\xi}, c(\boldsymbol{\xi})]$ , and hence  $H$ , is a linear functional of the salt concentration  $c(\boldsymbol{\xi})$ . One way to close the expression for  $H(\boldsymbol{\xi})$  is to assume that flow and transport are coupled only via the boundary condition at the saltwater boundary at  $\xi_1 = 1$ , i.e., to disregard the spatial variability of water density  $\rho$ . We refer to this approximation as the “decoupled” model (Simpson & Clement 2003). Its solution for the salt concentration

takes the form of the the Heaviside function  $\Theta$ ,

$$c_{\text{dec}}(\boldsymbol{\xi}) = \Theta(\xi_1 - 1 + \gamma), \quad (3.8)$$

where  $\gamma \ll 1$  is a model parameter. Substituting (3.8) into (3.5) – (3.7) and disregarding subleading contributions of order  $\gamma$  yields  $\eta_C = 0$  and a decoupled solution for the freshwater hydraulic head

$$H_{\text{dec}}(\boldsymbol{\xi}) = 1 - \xi_1 + \alpha \eta_B(\boldsymbol{\xi}). \quad (3.9)$$

We use a perturbation expansion in the coupling parameter  $\alpha$  to derive a solution for the fully coupled flow and transport problem (2.18) – (2.21) in the next section. As a prerequisite for such a solution, we first derive an integral equation for the transport problem (2.20) and (2.21).

### 3.2. Integral Equation for the Transport Problem

Substituting (3.5) into (2.20) leads to a transport equation

$$\frac{\partial c}{\partial \xi_1} - \beta \nabla^2 c = \alpha \nabla \eta_B \cdot \nabla c + \alpha \left( \nabla \eta_C \cdot \nabla + c \frac{\partial}{\partial \xi_3} \right) c. \quad (3.10)$$

Let  $g(\boldsymbol{\xi}, \boldsymbol{\xi}')$  be the Green's function defined as the solution of the advection-diffusion equation

$$\beta \nabla^2 g(\boldsymbol{\xi}, \boldsymbol{\xi}') - \frac{\partial g(\boldsymbol{\xi}, \boldsymbol{\xi}')}{\partial \xi_1} = -\delta(\boldsymbol{\xi} - \boldsymbol{\xi}'), \quad (3.11a)$$

subject to homogeneous boundary conditions

$$g|_{\xi_1=0} = g|_{\xi_1=1} = 0, \quad \frac{\partial g}{\partial \xi_3}|_{\xi_3=0} = \frac{\partial g}{\partial \xi_3}|_{\xi_3=c} = 0. \quad (3.11b)$$

Rewriting (3.10) in terms of  $\boldsymbol{\xi}'$ , multiplying the result with  $g(\boldsymbol{\xi}, \boldsymbol{\xi}')$ , integrating over  $\Omega_d$ , and applying the Green's theorem yields an integral equation

$$c(\boldsymbol{\xi}) = c_0(\boldsymbol{\xi}) + \alpha \int_{\Omega_d} g \nabla' \eta_B \cdot \nabla' c \, d\boldsymbol{\xi}' + \alpha \int_{\Omega_d} g \left( \nabla' \eta_C \cdot \nabla' + c \frac{\partial}{\partial \xi_3'} \right) c \, d\boldsymbol{\xi}'. \quad (3.12)$$

Here

$$c_0(\boldsymbol{\xi}) = \beta \int_{\partial \Omega_d} (g \nabla' c - c \nabla' g) \cdot \mathbf{dn} - \int_{\partial \Omega_d} c g \mathbf{e}_1 \cdot \mathbf{dn} \quad (3.13)$$

represents boundary effects on the salt concentration distribution  $c(\boldsymbol{\xi})$ . The second term on the right side of (3.12) reflects the influence of the hydrostatic saltwater boundary on salt transport, while the third contribution quantifies the linear coupling between flow and transport. Note that (3.13) is a solution of the transport problem (3.10) and (2.21) in the absence of density effects, i.e., when  $\alpha = 0$ .

We show in Appendix A.2 that for  $\xi_1' < \xi_1$  the Green's function  $g(\boldsymbol{\xi}, \boldsymbol{\xi}')$  is given by

$$g(\boldsymbol{\xi}, \boldsymbol{\xi}') = \exp\left(\frac{\xi_1 - \xi_1'}{2\beta}\right) \frac{2}{\beta \zeta} \sum_{m=0}^{\infty} c_m \cos\left(m\pi \frac{\xi_3}{\zeta}\right) \cos\left(m\pi \frac{\xi_3'}{\zeta}\right) \times \sinh[B_m \xi_1'] \frac{\sinh[B_m(1 - \xi_1)]}{B_m \sinh(B_m)}, \quad (3.14)$$

where  $c_0 = 1/2$ ,  $c_m = 1$  ( $m > 0$ ), and

$$B_m = \sqrt{\frac{1}{4\beta^2} + \left(\frac{m\pi}{\zeta}\right)^2}. \quad (3.15)$$

For  $\xi'_1 > \xi_1$ , the Green's function  $g(\boldsymbol{\xi}, \boldsymbol{\xi}')$  is obtained from (3.14) by switching the arguments  $\xi'_1$  and  $\xi_1$ . Substituting (3.14) into (3.13), while recalling boundary conditions (2.21), gives

$$c_0(\boldsymbol{\xi}) \equiv c_0(\xi_1) = \frac{\exp(\xi_1 \beta^{-1}) - 1}{\exp(\beta^{-1}) - 1}. \quad (3.16)$$

Since hydraulic head  $H(\boldsymbol{\xi})$  in (3.5) and salt concentration  $c(\boldsymbol{\xi})$  in (3.12) are coupled, the transport equation (3.10) is non-linear in  $c(\boldsymbol{\xi})$ . We solve this non-linear coupled problem analytically via a perturbation expansion in the coupling parameter  $\alpha$ .

#### 4. Perturbation Schemes

The coupling parameter  $\alpha$  compares a typical flow velocity induced by density contrasts at the saltwater boundary with the flow velocity without density effects. As such, its physical meaning is twofold. It measures the deviation of the flow velocity from uniform flow, i.e., from the  $x$ -coordinate, due to hydrostatic saltwater at the boundary  $\xi_1 = 1$ . Its magnitude is quantified by  $\eta_B(\boldsymbol{\xi})$  in (3.6). Furthermore,  $\alpha$  quantifies the influence of density effects on the flow velocity due to intruding saltwater. As such, it is a measure of the strength of the coupling between fluid flow and salt transport, as quantified by  $\eta_C[\boldsymbol{\xi}, c(\boldsymbol{\xi})]$  in (3.7).

For a weak coupling, i.e., for small  $\alpha$ , the integral equation (3.12) can be expanded into a perturbation series in powers of  $\alpha$ , which leads to

$$c(\boldsymbol{\xi}) = \sum_{k=0}^{\infty} \alpha^k c^{(k)}(\boldsymbol{\xi}). \quad (4.1)$$

Since  $\eta_C[\boldsymbol{\xi}, c(\boldsymbol{\xi})]$  given by (3.7) is linear in  $c(\boldsymbol{\xi})$ , it can be expanded as

$$\eta_C \left[ \boldsymbol{\xi}, \sum_{k=0}^{\infty} \alpha^k c^{(k)}(\boldsymbol{\xi}) \right] = \sum_{k=0}^{\infty} \alpha^k \eta_C \left[ \boldsymbol{\xi}, c^{(k)}(\boldsymbol{\xi}) \right]. \quad (4.2)$$

Thus, we obtain an expansion of hydraulic head  $H$  in the coupling parameter  $\alpha$ ,

$$H(\boldsymbol{\xi}) = \sum_{k=0}^{\infty} \alpha^k H^{(k)}(\boldsymbol{\xi}). \quad (4.3)$$

Substituting (4.2) into (3.5) gives an explicit expression for the expansion of  $H(\boldsymbol{\xi})$  in terms of the expansion of  $c(\boldsymbol{\xi})$  in (4.1),

$$H(\boldsymbol{\xi}) = 1 - \xi_1 + \alpha \left\{ \eta_B(\boldsymbol{\xi}) + \eta_C[\boldsymbol{\xi}, c^{(0)}(\boldsymbol{\xi})] \right\} + \sum_{k=2}^{\infty} \alpha^k \eta_C \left[ \boldsymbol{\xi}, c^{(k-1)}(\boldsymbol{\xi}) \right]. \quad (4.4)$$

The comparison of (4.3) and (4.4) shows that

$$\begin{aligned} H^{(0)}(\boldsymbol{\xi}) &= 1 - \xi_1, & H^{(1)}(\boldsymbol{\xi}) &= \eta_B(\boldsymbol{\xi}) + \eta_C \left[ \boldsymbol{\xi}, c^{(0)}(\boldsymbol{\xi}) \right], \\ H^{(k)}(\boldsymbol{\xi}) &= \eta_C \left[ \boldsymbol{\xi}, c^{(k-1)}(\boldsymbol{\xi}) \right], & k &> 1. \end{aligned} \quad (4.5)$$

Equations (4.5) reveal that the terms  $H^{(k)}(\boldsymbol{\xi})$  with  $k > 1$  in the expansion (4.3) depend on the terms  $c^{(k-1)}(\boldsymbol{\xi})$  in the expansion (4.1).

Substituting (4.1) and (4.2) into (3.12) yields

$$\begin{aligned} c(\boldsymbol{\xi}) &= c_0(\xi_1) + \sum_{k=1}^{\infty} \alpha^k \left\{ \int_{\Omega} g \nabla' \eta_B \cdot \nabla' c^{(k-1)} \, d\boldsymbol{\xi}' \right. \\ &\quad \left. + \sum_{m=0}^{k-1} \int_{\Omega} g \left( \nabla' \eta_C[\boldsymbol{\xi}', c^{(m)}] \cdot \nabla' + c^{(m)} \frac{\partial}{\partial \xi_3'} \right) c^{(k-m-1)} \, d\boldsymbol{\xi}' \right\}. \end{aligned} \quad (4.6)$$

The comparison of (4.1) and (4.6) reveals that  $c^{(0)}(\boldsymbol{\xi}) \equiv c_0(\xi_1)$  and, for  $k \geq 1$ ,

$$\begin{aligned} c^{(k)}(\boldsymbol{\xi}) &= \int_{\Omega} g \nabla' \eta_B \cdot \nabla' c^{(k-1)} \, d\boldsymbol{\xi}' \\ &\quad + \sum_{m=0}^{k-1} \int_{\Omega} g \left( \nabla' \eta_C[\boldsymbol{\xi}', c^{(m)}] \cdot \nabla' + c^{(m)}(\boldsymbol{\xi}') \frac{\partial}{\partial \xi_3'} \right) c^{(k-m-1)} \, d\boldsymbol{\xi}'. \end{aligned} \quad (4.7)$$

Thus our perturbation expansions generate a hierarchy of recursion relations for  $c^{(k)}(\boldsymbol{\xi})$ , which in turn determine the terms  $H^{(k+1)}(\boldsymbol{\xi})$  in the expansion of hydraulic head  $H(\boldsymbol{\xi})$ . As such, the fully coupled system of equations for flow and transport has been decoupled on the level of an expansion in the coupling parameter  $\alpha$ .

For the decoupled model (3.8) and (3.9), the transport equation (3.10) is linear in  $c(\boldsymbol{\xi})$ , the second term on the right-hand side of (4.7) is zero, and each  $c^{(k)}(\boldsymbol{\xi})$  ( $k \geq 1$ ) in (4.7) depends only on the lower-order expansion term  $c^{(k-1)}(\boldsymbol{\xi})$ . Hydraulic head  $H(\boldsymbol{\xi})$  is exact to first order in  $\alpha$  for the decoupled problem. In this case, the perturbation solution represents an expansion in the deviations of the exactly known flow field from constant uniform flow in the  $\xi_1$ -direction, and every approximation order increases the accuracy of a solution for salt concentration.

For the fully coupled model, the non-linearity of the transport equation (3.10), caused by the dependence of  $H$  on salt concentration, manifests itself through the dependence of the expansion terms  $c^{(k)}(\boldsymbol{\xi})$  ( $k \geq 1$ ) on all previous  $c^{(j)}(\boldsymbol{\xi})$  with  $j \in [1, \dots, k-1]$ . Here, every approximation order in  $\alpha$  simultaneously increases the accuracy of solutions for  $c$  and  $H$ . In other words, to every order of approximation, one determines a solution to a slightly modified flow and transport problem.

## 5. Flow and Transport Behavior

In the following, we evaluate expressions (4.1) and (4.3) to first order in  $\alpha$ . We consider both the decoupled and coupled flow and transport problems, and compare the results with numerical simulations obtained from SUTRA (Voss & Provost 2002). Since SUTRA is a well tested and widely used software, we treat the solutions computed by SUTRA as a yardstick.

### 5.1. First-Order Approximations and Numerical Simulations

For the decoupled problem, the expression for hydraulic head  $H(\boldsymbol{\xi})$  is exact to first-order in  $\alpha$  and given by (3.9). The first-order approximation of the salt concentration

distribution is given by

$$c(\boldsymbol{\xi}) = c_0(\xi_1) + \alpha \int_{\Omega_d} g \frac{\partial \eta_B}{\partial \xi'_1} \frac{\partial c_0}{\partial \xi'_1} d\boldsymbol{\xi}' + O(\alpha^2). \quad (5.1)$$

For the fully coupled problem, the first-order approximations of hydraulic head  $H(\boldsymbol{\xi})$  and salt concentration  $c(\boldsymbol{\xi})$  are given by

$$H(\boldsymbol{\xi}) = 1 - \xi_1 + \alpha \eta_B(\boldsymbol{\xi}) + \alpha \eta_C[\boldsymbol{\xi}, c_0(\xi)] + O(\alpha^2) \quad (5.2)$$

and

$$c(\boldsymbol{\xi}) = c_0(\boldsymbol{\xi}) + \alpha \int_{\Omega_d} g \frac{\partial \eta_B}{\partial \xi'_1} \frac{\partial c_0}{\partial \xi'_1} d\boldsymbol{\xi}' + \alpha \int_{\Omega_d} g \frac{\partial \eta_C[\boldsymbol{\xi}', c_0(\xi'_1)]}{\partial \xi'_1} \frac{\partial c_0}{\partial \xi'_1} d\boldsymbol{\xi}' + O(\alpha^2), \quad (5.3)$$

respectively. The coefficients  $b_l^{(1)}$  and  $b_l^{(2)}$  in the expression for  $\eta_C$  (3.7) are evaluated explicitly to yield

$$b_l^{(1)} \equiv b_l^{(2)} = 2 \frac{(-1)^l - 1}{[1 + (l\pi\beta)^2] l \pi [\exp(\beta^{-1}) - 1]} - 2 \frac{(-1)^l l \pi \beta^2}{1 + (l\pi\beta)^2}. \quad (5.4)$$

The infinite summations in the expressions for the Green's function  $g$  in (3.14),  $\eta_B$  in (3.6) and  $\eta_C$  in (3.7) converge exponentially with the summation index. Their numerical evaluations requires a relatively small number of terms (10, in our numerical calculations). The quadratures in (5.1) and (5.3) were evaluated numerically with a ten-point Gauss-Legendre integration (Press *et al.* 1992).

Direct numerical simulations of the flow and transport problems (2.18) – (2.21) were performed with SUTRA (Voss & Provost 2002), a finite element code for solving a time-dependent system of partial differential equations for variable-density flow and transport. The calculations for the decoupled and coupled transport problems were performed with a spatial resolution of  $\Delta \xi_1 = \Delta \xi_3 = 1/128$ , which corresponds to  $256 \times 128$  elements. For the decoupled problem, heads and concentrations were obtained by solving the steady-state flow and transport equations. For the coupled problem, heads and concentrations were determined iteratively as an asymptotic limit of the respective transient solutions. The solutions were asymptotically stationary and did not change after a simulation time of  $6 \times 10^5$  seconds.

## 5.2. Results

In the following simulations, we set an aperture  $\zeta = 0.5$  and the Peclet number  $\beta = 0.1$ . The former corresponds to the original shape of the flow domain in the Henry problem. The latter represents the Peclet number for which the intrusion of seawater is noticeable without being dominated by diffusion. We considered a range of values of the coupling parameter  $\alpha$  varying from  $\alpha = 0.25$  to 2.0. Since we set  $\epsilon = 1/40$ , the lowest value corresponds to a freshwater hydraulic head gradient of 10%, which should be considered as high, while the other extreme ( $\alpha = 2$ ) corresponds to a freshwater hydraulic head gradient of 1.25%, which is typical for many coastal aquifers.

### 5.2.1. Freshwater Head

Figure 2 illustrates the first-order solutions (3.9) and (5.2) for the decoupled and coupled flow and transport models, respectively. For weak coupling ( $\alpha = 0.25$  and 0.5), the solutions for hydraulic head  $H(\boldsymbol{\xi})$  resulting from the two models coincide at some distance from the saltwater boundary  $\xi_1 = 1$ , while differing significantly in the region adjacent to

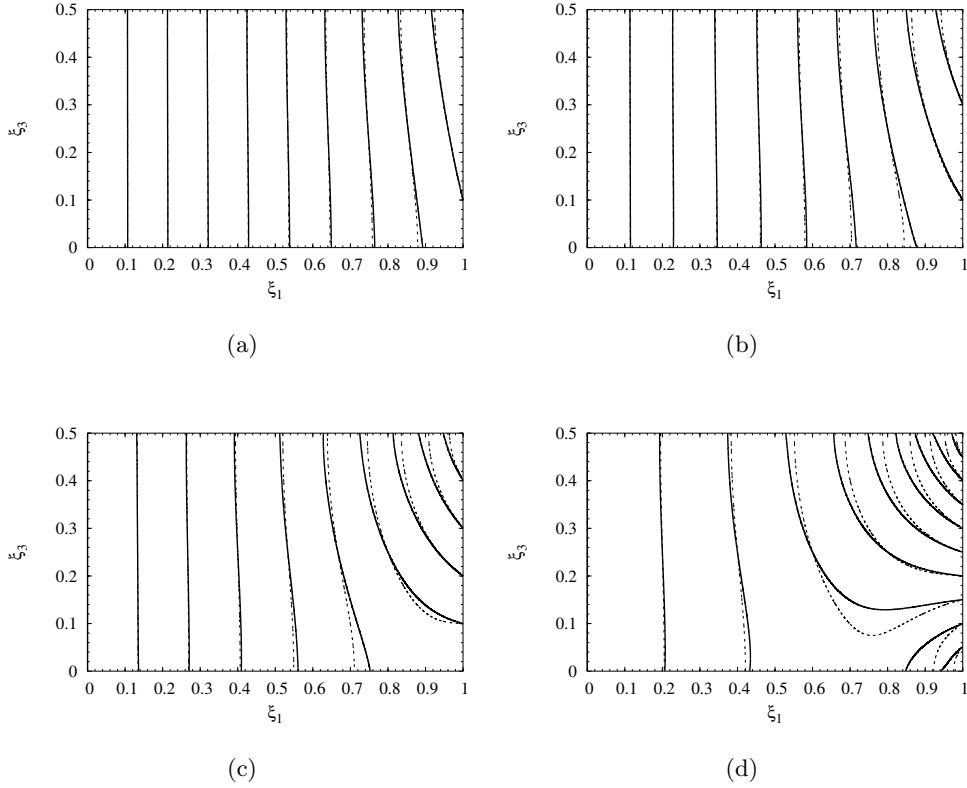


FIGURE 2. Equipotential lines of the first-order approximation of dimensionless freshwater head  $H(\boldsymbol{\xi})$  corresponding to the coupled model (solid lines) given by (5.2) and to the decoupled model (dashed lines) given by (3.9), for  $\zeta = 0.5$ ,  $\beta = 0.1$ , and (a)  $\alpha = 0.25$ , (b)  $\alpha = 0.5$ , (c)  $\alpha = 1.0$ , and (d)  $\alpha = 2.0$ . The isolines are equidistant with  $\Delta H = 0.1$ .

this boundary. Hydraulic head is dominated by the saltwater boundary conditions, yet visible density effects due to the intruding saltwater are apparent. The head isolines in the coupled model are more curved than their decoupled counterparts, which indicates an increasing vertical component of the flow velocity.

For a stronger coupling ( $\alpha = 1.0$  and  $2.0$ ), the differences between the head isolines for the two models become more pronounced. The distance between the isolines in the left half of the flow domain increases compared to the weaker coupling, which indicates a decreasing freshwater flow. In the upper right corner, the isolines become closer, which implies an increasing freshwater outflow. The head isolines connecting the bottom of the flow domain with the saltwater boundary indicate a convection cell developing in the lower right corner. For the coupled model, this convection cell intrudes more into the flow domain than for the decoupled model. Note that  $H(\boldsymbol{\xi})$  for the decoupled model is exact to first order in  $\alpha$ , as discussed in the previous section. The first-order approximation for the coupled model, however, is not expected to be consistent for such values of  $\alpha$ , because it is strictly valid only for a weak coupling. This issue is discussed below.

Figure 3 compares the head isolines obtained from the first-order approximation (5.2) of the coupled problem (solid lines) and from direct numerical simulations (dashed lines) of the full problem (2.18) – (2.21). (SUTRA simulations of the decoupled problem produce

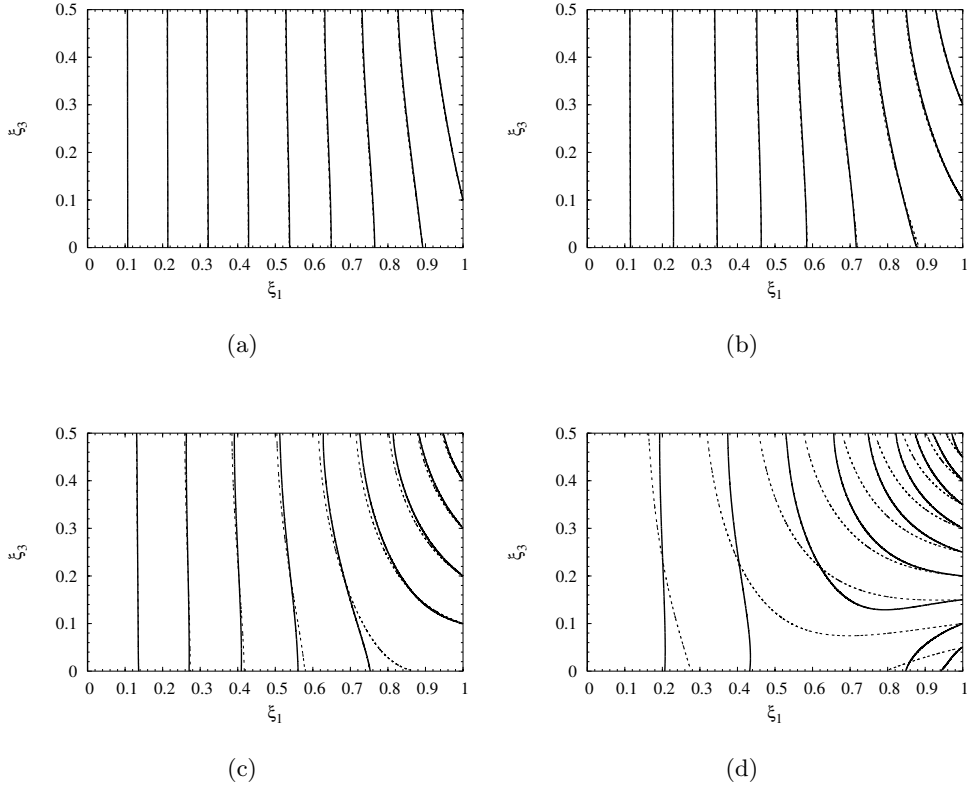


FIGURE 3. Equipotential lines of the first-order approximation of dimensionless freshwater head  $H(\boldsymbol{\xi})$  resulting from the coupled model (solid lines) given by (5.2) and of the numerical solution of the full problem (2.18) – (2.21) obtained with SUTRA (dashed lined), for  $\zeta = 0.5$ ,  $\beta = 0.1$ , and (a)  $\alpha = 0.25$ , (b)  $\alpha = 0.5$ , (c)  $\alpha = 1.0$ , and (d)  $\alpha = 2.0$ . The isolines are equidistant with  $\Delta H = 0.1$ .

solutions for freshwater heads that are identical to the exact analytical solution (3.9), and not displayed here.)

For weak coupling ( $\alpha = 0.25$  and  $0.5$ ), the head isolines obtained from the first-order approximation coincide with those obtained from SUTRA, confirming the consistency and accuracy of our perturbation solution. As  $\alpha$  increases, the first-order solution deviates from its numerical counterpart. For  $\alpha = 1$ , the first-order approximation remains fairly robust. The largest deviations from the numerical solutions are observed in the lower right half of the flow domain, close to the saltwater boundary. This is because the boundary conditions at the bottom and top of the flow domain are expressed by (2.18) and (3.7b) in terms of the salt concentration  $c(\boldsymbol{\xi})$ . The first-order approximation of  $c(\boldsymbol{\xi})$  is given by the “bare” solution  $c_0(\xi_1)$ , which is independent of  $\xi_3$ . However, saltwater intrusion is most pronounced in the lower right corner, where a convection cell develops resulting in a strong dependence on  $\xi_3$ . This feature is a higher-order effect and cannot be taken into account by the first-order approximation.

For strong coupling with  $\alpha = 2$ , the differences between the two solutions are significant and occur throughout the flow domain  $\Omega_d$ . The isolines of the full numerical solution are more curved than those given by the first-order approximation indicating larger vertical flow. On a separate note, Figure 3 shows that the extent of the convection cell increases

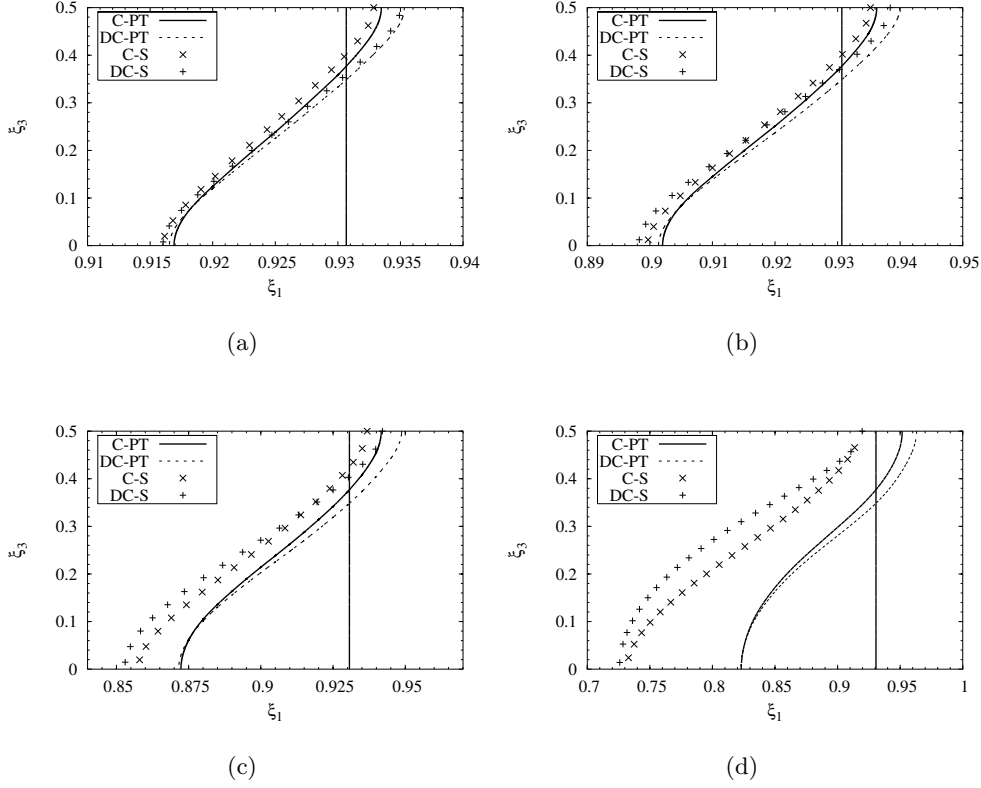


FIGURE 4. Isolines  $c(\boldsymbol{\xi}) = 0.5$  for the salt concentration given by the first-order solutions (5.3) and (5.1) of the coupled (C-PT) and decoupled (DC-PT) problems, respectively, as well as by direct numerical simulations with SUTRA for the coupled (C-S) and decoupled (DC-S) problems, for  $\zeta = 0.5$ ,  $\beta = 0.1$ , and (a)  $\alpha = 0.25$ , (b)  $\alpha = 0.5$ , (c)  $\alpha = 1.0$ , and (d)  $\alpha = 2.0$ . The vertical solid lines are the  $c_0(\xi_1) = 0.5$  isolines corresponding to the zeroth-order approximation of  $c(\boldsymbol{\xi})$ .

with the degree of coupling between the flow and transport processes, i.e., with increasing coupling parameter  $\alpha$ .

Of course, it should come as no surprise that the accuracy of the perturbation solution (5.2) deteriorates with increasing  $\alpha$ . Indeed, the use of  $\alpha$  as a (small) perturbation parameter formally limits the range of applicability of (5.2) to  $\alpha \ll 1$ . Nevertheless, Figure 3 demonstrates that the perturbation solution (5.2) for freshwater head  $H(\boldsymbol{\xi})$  remains accurate for moderate coupling with  $\alpha$  as high as 1.

### 5.2.2. Salt Concentration

Figure 4 shows the  $c(\boldsymbol{\xi}) = 0.5$  isolines for the salt concentration  $c(\boldsymbol{\xi})$  computed with the first-order approximations of analytical solutions of the coupled (5.3) and decoupled (5.1) problems, as well as with direct numerical simulations (SUTRA) of these problems. One can see how the heavier saltwater intrudes at the right bottom of the flow domain, while it is pushed back by the outflowing lighter freshwater at the right top.

For small to moderate coupling ( $\alpha = 0.25, 0.5$ , and 1), the bare solution  $c_0(\xi_1)$  significantly underestimates the extent of seawater intrusion in the lower two thirds of the flow domain, and underestimates it in the upper part of the flow domain. The first-order

approximations of both the coupled and decoupled problems qualitatively capture the behavior of the front. For strong coupling with  $\alpha = 2$ , the convection cell developing at the right bottom transports sufficient amounts of saltwater to the upper part of the flow domain to induce, together with diffusion as a transverse spreading mechanism, a deeper intrusion than it would for purely diffusive transport in uniform flow, as represented by  $c_0(\xi_1)$ . This higher-order feature is not captured by the first-order approximations.

For all  $\alpha$ , the difference between the coupled and decoupled concentration isolines is significant, and is reflected in the first-order solution. In the coupled model, saltwater intrudes consistently more at the top of the domain and less at the bottom than for the decoupled case. As saltwater intrudes, it loses energy due to diffusion of salt, a feature which is inherently connected to the coupled nature of flow and transport. As such it is not present in the decoupled model, and saltwater can intrude further. As  $\alpha$  increases, the intersection between the coupled and decoupled isolines moves upwards and the convexity of the decoupled isolines increases.

As  $\alpha$  becomes larger, coupling effects become more important, which leads to more pronounced differences between the decoupled and coupled solutions. These features are not completely accounted for by the first-order perturbation approximations because, as discussed in the end of Section 4, the low order in  $\alpha$  means the low order with respect to an approximation of the transport solution for the decoupled model, while in the coupled model it implies the low order with respect to a simultaneous approximation of the solutions for the flow and transport problems. The density effects leading to the above features are of higher order in  $\alpha$ .

For weak coupling with  $\alpha = 0.25$  and  $0.5$ , the first-order approximation of the coupled and decoupled solutions are in a good agreement with “true” solutions obtained by SU-TRA. The discrepancy between the first-order solutions and their numerical counterparts increases with  $\alpha$ , as should be expected from the perturbative nature of the former.

## 6. Summary and Conclusions

We analysed steady-state density-dependent flow and transport in homogeneous porous media, as described by the Henry problem. This setup is often used to represent seawater intrusion in coastal aquifers, wherein fresh water is discharged to the sea, while salt water is advected and diffused into the aquifer. In the process, a transition zone between fresh and saline water develops, thus endangering the quality of fresh groundwater. The coupling of flow and transport phenomena is caused by the dependence of water density on salt concentration in water. We used a perturbation analysis to derive analytical solutions for the spatial distributions of water potential and salt concentration. This allowed us to analyze the relative effects of various transport mechanisms, as well as the strength of coupling between flow and transport processes. We also compared our perturbative solutions to direct numerical simulations, which were used to test the accuracy of our perturbative approach.

Our analysis leads to the following major conclusions

- Dimensionless groups controlling the flow and transport processes are the Peclet number  $\beta$  and a coupling parameter  $\alpha$ . They quantify the relative effects of advection and diffusion, and the relative importance of density effects and boundary conditions, respectively. The coupling parameter  $\alpha$  is of fundamental importance in the perturbative scheme we adopt. Its physical relevance resides in that it measures the strength of the coupling between fluid flow and salt movement, as well as quantifies the deviation of the flow velocity driven by the sea-side boundary condition from a uniform flow condition.
- A solution of the Henry problem is developed by using a Green’s function approach.

Closure of the resulting system of coupled equations is attained for two scenarios: first, we assume that coupling of flow and transport is due only to the saltwater boundary condition at the seaside, while neglecting effects of density variations within the domain (we refer to this approximation as the decoupled scenario); second, we analyze a fully coupled problem (we refer to this as the coupled scenario).

- The governing equations are solved analytically by means of a perturbation expansion in the coupling parameter  $\alpha$ . The salient feature of the perturbative scheme is that it generates a hierarchy of recursive relationships governing the distributions of hydraulic head and salt concentration, which effectively decouples flow and transport problems at every approximation order.

- The meaning of the approximation order in  $\alpha$  is different in the two scenarios considered. When coupling is due only to the saltwater boundary conditions, hydraulic head is exact to first order (in  $\alpha$ ), while transport is linear and the solution for concentration at the  $k$ -th step depends only on the concentration at the previous approximations level,  $k - 1$ . For the fully coupled problem, the transport equation is nonlinear due to the linear coupling of flow and transport. As a consequence, the solution to a given order (in  $\alpha$ ) simultaneously increases the order of approximation of both hydraulic head and concentration fields.

- We developed explicit first-order expressions for the freshwater head and concentration distributions. For moderate density coupling ( $\alpha \leq 0.5$ ), these approximations of the solutions of the coupled flow and transport problem compare well with direct numerical simulations obtained from SUTRA . For increasing stronger coupling of flow and salt transport, higher-order contributions of the perturbation series gain importance and lead to deviations from the “true” numerical solution.

The developed perturbation formalism provides a systematic analytical tool for the analysis of stable density dependent flow problems and sheds new light on coupled flow and transport mechanism in homogeneous porous environments. This general methodology can be applied to a range of boundary value problems and is not restricted to the particular conditions considered here. Furthermore, it can be readily extended to include time-dependent flow and transport scenarios as well as the heterogeneity of porous media. As such, the presented analytical method can serve as the basis for a systematic investigation of the influence of ever present small-scale medium heterogeneities on effective large scale flow and transport.

## Acknowledgments

The work of D. T. was performed at Los Alamos National Laboratory (LA-UR 04-5497) under the auspices of the National Nuclear Security Agency of U.S. Department of Energy under contract W-7405-ENG-36. This work was supported in part by the U.S. Department of Energy under the DOE/BES Program in the Applied Mathematical Sciences, Contract KC-07-01-01, and in part by the LDRD Program at Los Alamos National Laboratory. M. D. gratefully acknowledges the financial support of the Spanish Secretaría de Estado de Educación y Universidades and the program ‘Ramon y Cajal’ of the Spanish Ministry of Science and Technology. The authors thank the Departament d’Universitat, Recerca i Societat de la Informació of the Catalan government for financial support.

## Appendix A. Green's Functions

In the following we derive the Green's functions for the flow problem in Section 3.1, and for the integral formulation of the transport problem in Section 3.2.

### A.1. Green Functions for the Flow Problem

The Green's function  $G(\boldsymbol{\xi}, \boldsymbol{\xi}')$  for (2.18) – (2.19) can be obtained by taking the limit of the Green's function for the corresponding time-dependent diffusion problem (Carslaw & Jaeger 1959),

$$G(\boldsymbol{\xi}, \boldsymbol{\xi}') = \frac{2}{\zeta \pi^2} \sum_{m=1}^{\infty} \frac{1}{m^2} \sin(m \pi \xi_1) \sin(m \pi \xi'_1) + \frac{4\zeta}{\pi^2} \sum_{m,n=1}^{\infty} \frac{1}{m^2 \zeta^2 + n^2} \sin(m \pi \xi_1) \sin(m \pi \xi'_1) \cos\left(n \pi \frac{\xi_3}{\zeta}\right) \cos\left(n \pi \frac{\xi'_3}{\zeta}\right). \quad (\text{A } 1)$$

This expression can be simplified by summing up the first sum on the right side and one of the double sums by using the relations,

$$2 \cos\left(n \pi \frac{\xi_3}{\zeta}\right) \cos\left(n \pi \frac{\xi'_3}{\zeta}\right) = \cos\left(n \pi \frac{\xi_3 + \xi'_3}{\zeta}\right) + \cos\left(n \pi \frac{\xi_3 - \xi'_3}{\zeta}\right), \quad (\text{A } 2)$$

$$2 \sin(m \pi \xi_1) \sin(m \pi \xi'_1) = \cos[m \pi (\xi_1 - \xi'_1)] - \cos[m \pi (\xi_1 + \xi'_1)], \quad (\text{A } 3)$$

and (Gradshteyn & Ryzhik 1980),

$$\sum_{n=1}^{\infty} \frac{1}{n^2 + \gamma^2} \cos\left(n \pi \frac{\xi}{b}\right) = \frac{\pi}{2\gamma} \frac{\cosh\left[\gamma \pi \left(1 - \frac{\xi}{b}\right)\right]}{\sinh(\gamma \pi)} - \frac{1}{2\gamma^2}, \quad (\text{A } 4)$$

$$\sum_{m=1}^{\infty} \frac{1}{m^2} \cos\left(m \pi \frac{\xi}{a}\right) = \frac{\pi^2}{6} - \frac{\pi^2 |\xi|}{2a} + \frac{\pi^2 \xi^2}{4a^2}. \quad (\text{A } 5)$$

Applying (A 2) and (A 4) to the second term on the right side of (A 1) and defining  $\gamma \equiv m \zeta$ , we obtain

$$\sum_{m=1}^{\infty} \sin(m \pi \xi_1) \sin(m \pi \xi'_1) \times \left\{ \frac{\cosh\{m \pi [\zeta - (\xi_3 + \xi'_3)]\} + \cosh[m \pi (\zeta - |\xi_3 - \xi'_3|)]}{\pi m \sinh(m \pi \zeta)} - \frac{2}{\zeta \pi^2 m^2} \right\}. \quad (\text{A } 6)$$

The third term on the right side of (A 6) cancels with the first term on the right side of (A 1), which yields representation (3.3) of the Green's function (A 1).

To derive an alternative representation for the Green function  $G(\boldsymbol{\xi}, \boldsymbol{\xi}')$ , we consider the first and second sums on the right side of (A 1) separately. Applying (A 3) and (A 5) to the first sum on the right side of (A 1) gives

$$\frac{2}{\zeta \pi^2} \sum_{m=1}^{\infty} \frac{1}{m^2} \sin(m \pi \xi_1) \sin(m \pi \xi'_1) = \frac{(\xi_1 + \xi'_1) - |\xi_1 - \xi'_1|}{2\zeta} - \frac{\xi_1 \xi'_1}{\zeta}. \quad (\text{A } 7)$$

Applying (A 3) and (A 4) to the second expression and defining  $\gamma \equiv n/\zeta$  yields

$$\sum_{n=1}^{\infty} \cos\left(n\pi \frac{\xi_3}{\zeta}\right) \cos\left(n\pi \frac{\xi'_3}{\zeta}\right) \times \frac{1}{\pi n \sinh(n\pi/\zeta)} \left\{ \cosh\left[n\pi \left(\frac{1}{\zeta} - \frac{|\xi_1 - \xi'_1|}{\zeta}\right)\right] - \cosh\left[n\pi \left(\frac{1}{\zeta} - \frac{\xi_1 + \xi'_1}{\zeta}\right)\right] \right\} \quad (\text{A } 8)$$

Combining (A 7) and (A 8) leads to representation (3.4).

### A.2. Green's Function for the Transport Problem

Following Morse & Feshbach (1953), we replace (3.11) with

$$\nabla^2 \varphi(\boldsymbol{\xi}) - \beta^{-1} \frac{\partial \varphi(\boldsymbol{\xi})}{\partial \xi_1} = -\frac{\rho(\boldsymbol{\xi})}{\beta} \quad (\text{A } 9)$$

and set

$$\varphi(\boldsymbol{\xi}) = \sum_{m=1}^{\infty} F_m(\xi_1) \cos\left(m\pi \frac{\xi_3}{\zeta}\right) + \frac{F_0(\xi_1)}{2}, \quad (\text{A } 10)$$

$$\rho(\boldsymbol{\xi}) = \sum_{m=1}^{\infty} \rho_m(\xi_1) \cos\left(m\pi \frac{\xi_3}{\zeta}\right) + \frac{\rho_0(\xi_1)}{2}, \quad (\text{A } 11)$$

where the  $F_m(\xi_1)$  are as yet unknown functions, and

$$\rho_m(\xi_1) = \frac{2}{\zeta} \int_0^{\zeta} \rho(\boldsymbol{\xi}) \cos\left(m\pi \frac{\xi_3}{\zeta}\right) d\xi_3. \quad (\text{A } 12)$$

Substituting (A 10) and (A 11) into (A 9) yields

$$\frac{d^2 F_m}{d\xi_1^2} - \left(\frac{m\pi}{\zeta}\right)^2 F_m - \frac{1}{\beta} \frac{dF_m}{d\xi_1} = -\frac{\rho_m(\xi_1)}{\beta}. \quad (\text{A } 13)$$

A solution of (A 13) is given by

$$F_m(\xi_1) = y_1(\xi_1) \left[ c_1 + \int \frac{\rho_m(\xi'_1) y_2(\xi'_1)}{\beta \Delta(y_1, y_2)} d\xi'_1 \right] + y_2(\xi_1) \left[ c_2 - \int \frac{\rho_m(\xi'_1) y_1(\xi'_1)}{\beta \Delta(y_1, y_2)} d\xi'_1 \right], \quad (\text{A } 14)$$

where the constants of integration  $c_1$  and  $c_2$  are determined from the boundary conditions, and  $\Delta(y_1, y_2)$  is the Wronski determinant for two independent solutions of the homogeneous problem (A 13). Such solutions are

$$y_1(\xi_1) = \exp\left(\frac{\xi_1}{2\beta}\right) \sinh(B_m \xi_1) \quad (\text{A } 15)$$

$$y_2(\xi_1) = \exp\left(-\frac{1-\xi_1}{2\beta}\right) \sinh(B_m (1-\xi_1)) \quad (\text{A } 16)$$

$$B_m \equiv \sqrt{\frac{1}{4\beta^2} + \left(\frac{m\pi}{\zeta}\right)^2}. \quad (\text{A } 17)$$

and the corresponding Wronski determinant is

$$\Delta(y_1, y_2) = -\exp\left(\frac{\xi_1}{2\beta}\right) \exp\left(-\frac{1-\xi_1}{2\beta}\right) B_m \sinh(B_m), \quad (\text{A } 18)$$

Substituting (A 15), (A 16) and (A 18) into (A 14) and adjusting the limits of integration to satisfy the boundary conditions, we obtain

$$F_m(\xi_1) = \int_0^1 \rho_m(\xi'_1) g_m(\xi_1, \xi'_1) d\xi'_1, \quad (\text{A } 19)$$

where

$$g_m(\xi_1, \xi'_1) = \frac{\exp\left(\frac{\xi_1 - \xi'_1}{2\beta}\right)}{\beta B_m \sinh(B_m)} \times \begin{cases} \sinh(B_m \xi_1) \sinh(B_m (1 - \xi'_1)) & \xi'_1 > \xi_1 \\ \sinh(B_m \xi'_1) \sinh(B_m (1 - \xi_1)) & \xi_1 > \xi'_1 \end{cases}. \quad (\text{A } 20)$$

Substituting (A 11), (A 12) and (A 19) into (A 10) leads to

$$\varphi(\boldsymbol{\xi}) = \int_0^1 d\xi'_1 \int_0^\zeta d\xi'_3 \rho(\boldsymbol{\xi}') \frac{2}{\zeta} \sum_{m=0}^{\infty} c_m g_m(\xi_1, \xi'_1) \cos\left(m\pi \frac{\xi_3}{\zeta}\right) \cos\left(m\pi \frac{\xi'_3}{\zeta}\right) \quad (\text{A } 21)$$

$$= \int_0^1 d\xi'_1 \int_0^\zeta d\xi'_3 \rho(\boldsymbol{\xi}') g(\boldsymbol{\xi}, \boldsymbol{\xi}'), \quad (\text{A } 22)$$

where  $c_m = 1/2$  for  $m = 0$  and  $c_m = 1$  else. Thus we obtain (3.14) for the Green's function  $g(\mathbf{x}, \mathbf{x}')$ .

#### REFERENCES

- ABARCA, E., CARRERA, J., HELD, R., SANCHEZ-VILA, X., DENTZ, M., KINZELBACH, W. & VAZQUEZ-SUÑE, E. 2004 Effective dispersion in seawater intrusion through heterogeneous aquifers. Book of extended synopses of 18th Salt Water Intrusion Meeting, Cartagena, May, 31–June,3, 2004.
- ALIEWI, A. S., MACKAY, R., JAYYOUSI, A., NASEREDDIN, K., MUSHTAHA, A. & YAQUBI, A. 2001 Numerical simulation of the movement of saltwater under skimming and scavenger pumping in the Pleistocene aquifer of Gaza and Jericho areas, Palestine. *Transp. Porous Media* **43** (1), 195 – 212.
- ALKALALI, A. & ROSTRON, B. 2003 Basin-scale analysis of variable-density groundwater flow: Nisku Aquifer, Western Canadian Sedimentary Basin. *J. Geochemical Exploration* **78** (9), 313 – 316.
- BEAR, J. 1972 *Dynamics of fluids porous media*. New York: Elsevier.
- BEAR, J., CHENG, A. H.-D., SOREK, S., OUAZAR, D. & HERRERA, I., ed. 1999 *Seawater Intrusion in Coastal Aquifers – Concepts, Methods, and Practices*. Dordrecht: Kluwer Academic Publishers.
- BEAR, J. & DAGAN, G. 1964 Some exact solutions of interface problems by means of the hodograph method. *J. Geophys. Res.* **69**, 1563 – 1572.
- CARSLAW, H. S. & JAEGER, J. C. 1959 *Conduction of heat in solids*, 2nd edn. New York: Oxford Univ. Press.
- CROUCHER, A. E. & O'SULLIVAN, M. J. 1995 The Henry problem for saltwater intrusion. *Water Resour. Res.* **31** (7), 1809 – 1814.
- CUSTODIO, E., BRUGGEMAN, G. A. & COTECCHIA, V. 1987 *Groundwater Problems in Coastal Areas, Stud. and Rep. in Hydrol.*, vol. 35. Paris: UNESCO.
- DIERSCH, H. G., AND O. KOLDITZ, 2002 Variable-density flow and transport in porous media: approaches and challenges. *Adv. Water Resour.* **25**, 899–944.
- GALEATI, G., GAMBOLATI, G. & NEUMAN, S. P. 1992 Coupled and partially coupled Eulerian-Lagrangian model of fresh-water-seawater mixing. *Water Resour. Res.* **28** (1), 149 – 165.
- GRADSHTEYN, I. S. & RYZHIK, I. M. 1980 *Table of integrals, series, and products*. New York: Academic Press.

- HENRY, H. R. 1964 Effects of dispersion on salt encroachment in coastal aquifers. *Tech. Rep.* Water Supply Pap. 1613-C. U. S. Geol. Surv.
- HERBERT, A. W., JACKSON, C. P. & LEVER, D. A. 1988 Coupled groundwater flow and solute transport with fluid density strongly dependent upon concentration. *Water Resour. Res.* **24** (10), 1781 – 1795.
- HOLZBECHER, M. E. 1998 *Modeling Density-Driven Flow in Porous Media*. Heidelberg/New York: Springer.
- HUPPERT, H. E. & WOODS, A. W. 1995 Gravity-driven flows in porous layers. *J. Fluid Mech.* **292**, 55 – 69.
- KACIMOV, A. R. & OBNOSOV, Y. V. 2001 Analytical solution for a sharp interface problem in sea water intrusion into a coastal aquifer. *Proc. Royal Soc. London, Series A* **457** (2016), 3023 – 3038.
- MANICKAM, O. & HOMS, G. M. 1995 Fingering instabilities in vertical miscible displacement flows in porous media. *J. Fluid Mech.* **288**, 75 – 102.
- MORSE, P. M. & FESHBACH, H. 1953 *Methods of Theoretical Physics*. New York: McGraw Hill.
- NAJI, A., CHENG, A. H.-D. & OUAZAR, D. 1998 Analytical stochastic solutions of saltwater/freshwater interface in coastal aquifers. *Stoch. Hydrol. Hydraul.* **12**, 413 – 429.
- OLTEAN, C., FELDER, C., PANFILOV, M. & BUES, M. A. 2004 Transport with a very low density contrast in Hele-Shaw cell and porous medium: Evolution of the mixing zone. *Transp. Porous Media* **55** (3), 339 – 360.
- OPHORI, D. U. 2004 A simulation of large-scale groundwater flow and travel time in a fractured rock environment for waste disposal purposes. *Hydrogeological Processes* **18** (9), 1579 – 1593.
- PANDAY, S., HUYAKORN, P. S., ROBERTSON, J. B. & MCGURK, B. 1993 A density-dependent flow and transport analysis of the effects of groundwater development in a fresh-water lens of limited areal extent - The Geneva area (Florida, USA) case study. *J. Contaminant Hydrol.* **12** (4), 329 – 354.
- PANICONI, C., KHLAIFI, I., LECCA, G., GIACOMELLI, A. & TARHOUNI, J. 2001 Modeling and analysis of seawater intrusion in the coastal aquifer of eastern Cap-Bon, Tunisia. *Transp. Porous Media* **43** (1), 3 – 28.
- PINDER, G. F. & COOPER, H. H. 1970 A numerical technique for calculating transient position of saltwater front. *Water Resour. Res.* **6** (3), 875 – 882.
- PRESS, W. H., TEUKOLSKY, S. A., VETTERLING, W. T. & FLANNERY, B. P. 1992 *Numerical Recipes in C, Second Edition*. Cambridge University Press.
- SCHELKES, K., VOGEL, P. & KLINGE, H. 2001 Density-dependent groundwater movement in sediments overlying salt domes. The Gorleben site example. *Physics and Chemistry of the Earth Part B - Hydrology, Oceans and Atmosphere* **26** (4), 361 – 365.
- SCHINCARIOL, R. A. & SCHWARTZ, F. W. 1990 An experimental investigation of variable density flow and mixing in homogeneous and heterogeneous media. *Water Resour. Res.* **26** (10), 2317 – 2329.
- SEGOL, G. 1994 *Classic groundwater simulations – proving and improving numerical models*. Englewood Cliffs, Prentice Hall.
- SEGOL, G., PINDER, G. F. & GRAY, W. G. 1975 Galerkin-finite element technique for calculating transient position of saltwater front. *Water Resour. Res.* **11** (2), 343 – 347.
- SIMMONS, C. T., NARAYAN, K. A., WOODS, J. A. & HERCZEG, A. L. 2002 Groundwater flow and solute transport at the Mourquong saline-water disposal basin, Murray Basin, southeastern Australia. *Hydrogeol. J.* **10** (2), 278 – 295.
- SIMPSON, M. J. & CLEMENT, T. P. 2003 Theoretical analysis of the worthiness of Henry and Elder problems as benchmarks of density-dependent groundwater flow models. *Adv. Water Resour.* **26** (1), 17 – 31.
- SMITH, A. J. & TURNER, J. V. 2001 Density-dependent surface water-groundwater interaction and nutrient discharge in the Swan-Canning Estuary. *Hydrol. Processes* **15** (13), 2595 – 2616.
- TAYLOR, T. P., PENNELL, K. D., ABRIOLO, L. M. & DANE, J. H. 2001 Surfactant enhanced recovery of tetrachloroethylene from a porous medium containing low permeability lenses — 1. Experimental studies. *J. Contaminant Hydrology* **48** (3-4), 325 – 350.
- VOSS, C. I. & PROVOST, A. M. 2002 SUTRA, A model for saturated-unsaturated variable-

- density ground-water flow with solute or energy transport. *Tech. Rep.* Water-Resources Investigations Report 02-4231. U.S. Geological Survey.
- WEATHERILL, D., SIMMONS, C. T., VOSS, C. I. & ROBINSON, N. I. 2004 Testing density-dependent groundwater models: two-dimensional steady state unstable convection in infinite, finite and inclined porous layers. *Adv. Water Resour.* **27** (5), 548 – 563.
- WOODING, R. A., TYLER, S. W. & WHITE, I. 1997 Convection in groundwater below an evaporating salt lake. 1. Onset of instability. *Water Resour. Res.* **33**, 1199 – 1217.
- YANG, J. W. & EDWARDS, R. N. 2000 Predicted groundwater circulation in fractured and unfractured anisotropic porous media driven by nuclear fuel waste heat generation. *Canadian J. Earth Sci.* **37** (9), 1301 – 1308.